View metadata, citation and similar papers at core.ac.uk
brought to you by CORE
provided by NOPR

Indian Journal of Pure & Applied Physics
Vol. 58, September 2020, pp. 667-672

Photon irradiation effects on electrical properties of *n*-ZnO/*p*-Si junctions for optoelectronic device

Shivangi S Patel, Bhaumik V Mistry, Sushant Zinzuvadiya & U S Joshi*
Department of Physics, School of Science, Gujarat University, Ahmedabad 380 009

Received 10 October 2019; accepted 14 July 2020

Simple high energy laser photon irradiation is a handy tool to tune the functional properties of wide band gap oxide-based devices. Present study reports on the effects of laser photon irradiation on electrical transport behaviour of *n*-ZnO/*p*-Si *p-n* junctions. The *n*-type conductivity of ZnO was optimised by doping of stoichiometric amount of Al in ZnO. The *n*-ZnO/*p*-Si junctions were grown on *p*-Si (100) substrate by pulsed laser deposition. The structural property was analysed by X-ray diffraction. Morphological study was done using atomic force microscopy (AFM) which shows smooth and mono-dispersed surfaces of the *p-n* junction. The current-voltage (*I-V*) characteristic of the *n*-ZnO/*p*-Si devices have been measured at room temperature in the dark and under illumination. Moreover, the effects of 532 nm visible laser light irradiation on the electric parameter of *n*-AZO/*p*-Si *p-n* junctions were investigated. The characteristic parameters of the junctions such as barrier height, ideality factor and series resistance were determined from the current-voltage measurement. The results show a promise of ZnO based diode structure for its optoelectronic applications.

Keywords: ZnO, Pulse laser deposition, photon irradiation, optoelectronic devices

Introduction

Zinc oxide has a multipurpose characteristics which include wide and direct band gap (3.37eV), high exciton binding energy, high electron mobility and low loss plasmonic material properties[1-3]. Heterojunction thin films possess several potential advantages like an excellent blue light response, simple processing steps, and low processing temperature[4–6] of a wide band gap transparent conductive oxide (TCO) on a single crystal silicon (Si) wafer[7]. The hybrid *n*-ZnO/*p*-Si junctions have advantage in optoelectronic devices because of large exciton binding energy of ZnO and low cost of Si wafer[8-9]. However, there are very few reports on PLD grown AZO film on Si substrate of the *n*-Al doped ZnO/*p*-Si junction and irradiated by photons[10]. Energetic irradiation with low or soft beam to heavy ion beams offers several advantages in not only understanding the basic physics governing the mechanism of a given property but also in tuning the functional properties of devices[4-6,11-12]. Modification of surface properties plays a crucial role in optimizing material's behaviour for a given application[13-14]. The multi scale surface modification is a challenging factor for the development of new materials. The unique interaction of laser light with a material can lead to permanent changes in the material's properties not easily achievable through other means. Laser irradiation can induce changes to the local chemistry, the crystal structure, and morphology, all of which affect the material behaviour for a given application[15-16]. The primary objective of the current work was to study optoelectronic properties of *n*-ZnO/*p*-Si junctions irradiated by energetic photon beams.

Experimental procedure

For the pulse laser deposition of thin film, ceramic target of AZO was fabricated through solid state reaction method. High-purity (99.9%) powders of ZnO and Al_2O_3 were used in stoichiometric amount for 2% Al doped in ZnO target[17]. The diameter and thickness of the AZO target was 15 mm and 5 mm respectively.Thin film of the AZO on *p*-Si was grown by PLD technique using Nd:YAG laser (EKSPLA, Model-NL303,Lithuania)[18]. The pulses of Nd:YAG laser (λ= 355mm, pulse width 5ns, repetition rate 10Hz) having 3rd harmonic (240 mJ power) was focused through a spherical lens on targets at 45º incidence. In order to achieve uniform ablation, the target was rotated during laser ablation. The substrates were set parallel to the target at a distance of 4 cm. Prior to deposition, the chamber was evacuated to 8.5×10^{-7} mbar pressure. Silicon wafer was first ultrasonically cleaned with acetone, ethanol

Corresponding author: (E-mail: usjoshi@gmail.com)

and deionised water. Many researchers have found that the electrical properties strongly depend on the thickness of ZnO films for application in optoelectronic devices[18-20]. The optimum film thickness should be chosen for the best device performance. About 150 nm thick Al-ZnO thin films was obtained. Next, the *n*-ZnO/*p*-Si junction was irradiated with laser light using Q-switched Nd:Yag laser operating in visible light (λ = 532 nm) having energy of 2.33 eV which is well below the energy that binds together the ZnO lattice (~7.5 eV) and the laser beam was focused using converging optics. The fluence is adjusted by keeping laser power at 1 J/cm^2. In the experiment, 5 laser pulses with a spot size of about 1 mm were made incident at the same point due to the non-uniform spatial distribution and 10 % stability of the pulse energy.

The *n*-ZnO/*p*-Si junctions were characterized by studying structural, electrical and optical properties. Grazing Incidence X-ray diffraction (GIXRD) of the films was performed with PANalytical XPert PRO system with Cu-kα radiation (λ= 1.54Aº). The thickness of the thin films was measured by a stylus profiler (Dektak 6 M). The surface morphology of the film was investigated by atomic force microscopy (AFM) (Nanosurf, EasyScan2). The optical spectroscopy was performed by using UV-VIS- NIR spectrophotometer (Shimadzu, UV-2600).Transport properties of the charge carriers were studied by Hall Effect measurement in the van der Pauw geometry (Ecopia, HMS-3000). The current voltage characteristics of pristine and photon irradiated *p-n* junctions were performed at room temperature in different light illumination using Keithley 2450 system source meter.

Result and Discussion

Typical GIXRD pattern of the *n*-ZnO/*p*-Si structure is shown in Fig. 1. XRD measurements revealed that AZO film on silicon substrate was polycrystalline. Due to preferential orientation of silicon (100) substrate, The AZO film also grow in (100) direction and hence the (100) peak is dominant for AZO thin film. The (100), (002), (110) and (201) peaks for AZO at 32.59º, 35.310º, 57.680º and 68.976 º of 2θ agree with the standard JCPDF file No 89-0510. This all peaks are well match to the pure ZnO hexagonal wurtzite phase.[21]

The average crystallite size was determined from Scherer formula

$$D = \frac{0.94\lambda}{\beta cos\theta}$$

where, D is the crystallite size, k is the shape factor lying between 0.95 and 1.15 depending on the shape of the crystals and in the present study the value is assumed to be 1, β is the full width at half maximum (FWHM) of the diffraction peak in radians, h is the Braggangle of the diffraction peak and λ is the wavelength of X-rays. The prominent peak (100) was used to calculate the crystallite size. The average crystallite size as calculated from XRD was found to be 12 nm for the AZO films.

Fig. 2 shows (a) 2D and (b) 3D AFM images of AZO thin film deposited on Silicon substrate. Uniform grain distribution can be seen in the AFM and the average particle size estimated from the AFM image lies in the range of 12 to 16 nm for the AZO film which agrees with that estimated from the XRD. The RMS roughness of the AZO film grown on Si was 5.57 nm calculated from the AFM image analysis.

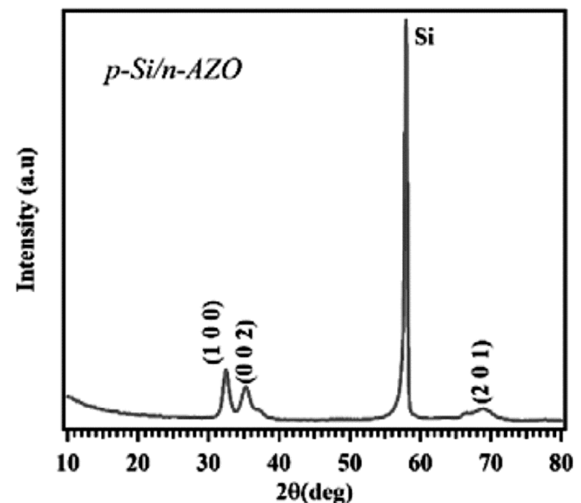

Fig. 1 — GIXRD image of *n*-ZnO/*p*-Si junction.

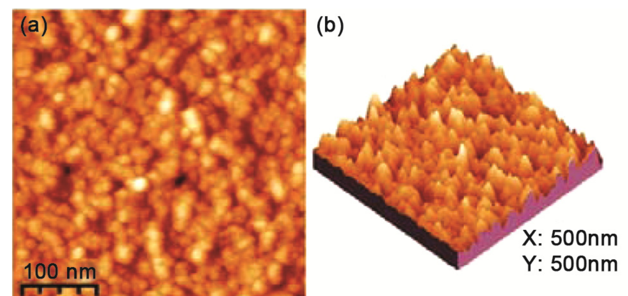

Fig. 2 — (a) 2-dimensional and (b) 3-dimensional AFM image of AZO thin film grown on Si.

The elemental analysis of *n*-ZnO/*p*-Si junction was done by using EDAX measurement. Fig. 3 shows the EDX spectra of *n*-ZnO/*p*-Si device, which reveals the existence of Si, Zn, O and Al elements on the AZO/Si film surface. The atomic Al doping ratio is found to be 2.20 which indicate the Al/Zn atomic ratios in film and bulk pallet are nearly same and confirms the reliability of pulsed laser deposition technique.

Optical properties of AZO thin films were investigated by UV-VIS-NIR spectrophotometer. Fig. 4 shows transmittance spectra in the wavelength range 200-900 nm for AZO thin film deposited on glass substrate with same deposition parameter as that deposited on silicon substrate. The transparency of AZO thin film is more than 85% in the visible range and which very good for transparent conducting oxides. Optical band gap energies were calculated by absorption co efficient (α) and incident energy of photon ($h\nu$) using Tauc equation[22]

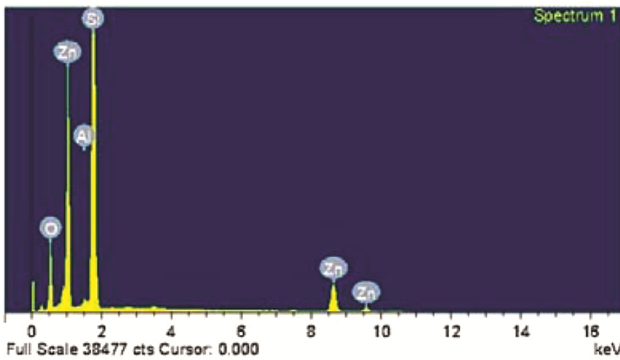

Fig. 3 — EDX spectra of *n*-ZnO/*p*-Si junction.

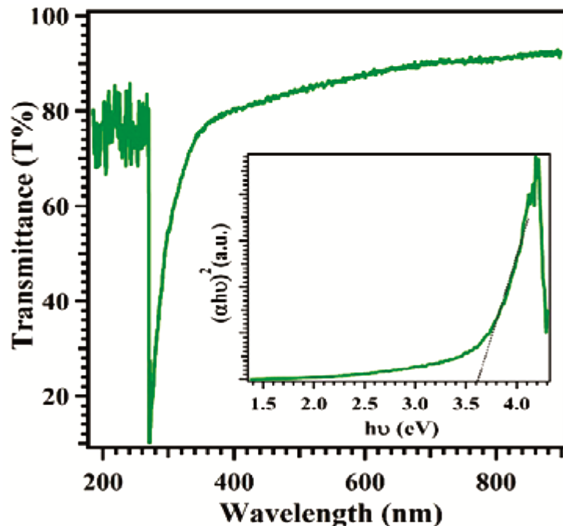

Fig. 4 — (a) Optical transmittance spectra and Band gap calculation plot (inset) of AZO thin film.

$$\left(\alpha h\nu = k(h\nu - E_g)^{\frac{1}{2}}\right)$$

Where, α is the absorption coefficient, $h\nu$ is energy, k is a constant and E_g is the optical band gap energy. The plot of $(\alpha h\nu)^2$ versus $h\nu$ is shown as the inset of fig.4; which on extrapolating the linear portion to energy axis at α=0 gives the band gap energy value. The optical band gap of the AZO thin film was calculated from graph is 3.6eV.

Hall Effect measurement was carried out with the help of Hall Effect measurement system (Ecopia corp., HMS-3000). The carrier concentration, resistivity and Hall mobility of AZO thin film were estimated to be 7.6×10^{19} cm^{-3}, 4.049×10^{-1} Ωcm and 1.9 $cm^2V^{-1}S^{-1}$, respectively. The negative sign of Hall co-efficient indicates that AZO thin film is *n*-type conducting film.

For electrical measurements, Al electrodes of dimension 400×200 μm^2 were deposited through metal shadow mask by vacuum evaporation on *p*-Si for bottom electrode and on AZO for top electrode. Gold probes were pressed directly on the films for electrical contacts. Typical two wire technique was employed to study the current voltage (*I-V*) characteristic of *n*-AZO/*p*-Si *p-n* junction diode using Keithley 2450 system source meter. The schematic of electrical measurement geometry of the *n*-ZnO/*p*-Si junction is displayed in fig. 5(a).

Fig. 5(b-c) shows the *I-V* characteristics of *n*-ZnO/*p*-Si junction recorded at room temperature by continuous voltage sweep and currents were measured in step of 0.01 V. The *I-V* characteristics show rectifying properties indicting proper formation of the junction. The electric measurements were done in three different light spectrum conditions, to examine

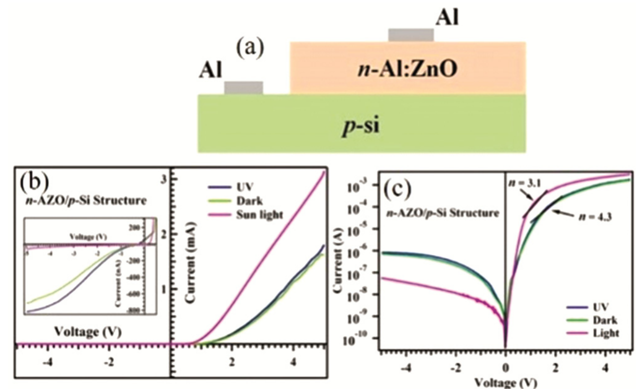

Fig. 5 — (a) Schematic of *n*-ZnO/*p*-Si junction with Al electrodes for electric measurement, (b) Typical *I–V* characteristics of *n*-ZnO/*p*-Si junctions linear four quadrant and (c) semi log *I-V* plots recorded under sun light, dark and UV illuminated junctions.

the optoelectronic nature of the *p-n* junctions. The *I-V* characteristics were recorded under ambient light condition, ultra-violet illumination and under dark condition (no light).

The current in forward bias is affected by the light condition. The inset of the fig. 5 (b) shows the reverse bias *I-V* sweep of the *p-n* junction indicates the very small leakage current for negative bias voltage in all conditions. The turn on voltage was obtained around 0.8 V under normal light condition whereas for dark and ultraviolet illumination condition the turn on voltage is 1.2 V.

The turn on voltage, ideality factor, saturation current density and forward to reverse bias currents were calculated to determine the diode characteristics. The standard diode equation can be written as[23]

$$I = I_S exp\left[\left(\frac{qV}{nkT}\right) - 1\right]$$

Where I_S is the saturation current, k is the Boltzmann constant, T is the absolute temperature, q is the electronic charge, V is the applied voltage, I is the diode current and n is the ideality factor. To obtain the ideality factor at a low forward bias, we plotted *I-V* curves as *ln I-V* and is shown in the fig. 5(c). The ideality factors were obtained from the slope of the *ln I-V* curves using following equation.

$$n = \frac{q}{kT}\left(\frac{dV}{d(lnI)}\right)$$

The saturation current density was obtained from the straight-line intercepts of the *ln I-V* curves at V=0. Forward-to-reverse current ratio was 1.47×10^3 at ± 5 V for normal light condition; whereas it was 2.26×10^3 at ± 5 V for dark and ultraviolet light condition. The electrical parameters evaluated from the *I-V* characteristics under different conditions are tabulated in Table 1. This *p-n* junction can be used in photo-detector application. The performance of the UV photo-detector is usually evaluated by photo-to-dark current ratio (PDCR), which can be measured using the formula as follows[24],

$$PDCR = (I_p - I_d)/I_d$$

Where, I_d is the dark current and I_p is the photocurrent under UV-illumination. The PDCR of n-ZnO/p-Si under 5.0 V reverse bias are then calculated to be 0.46. Under the reverse bias conditions, the photocurrent caused by the AZO surfaces by exposing under the light is obviously much larger than the dark current. The AZO film is highly transparent (T > 90%) in the visible region. The visible light passes through the AZO film and is absorbed primarily by the underlying *p*-Si. Thus, photon-induced electron–hole pairs are created only in the Si substrate at the region close to the interface where the recombination of the carriers can be neglected, and then are separated by the built-in electric field at the interface of the junction, which results in the observed photocurrent under the reverse bias conditions[6]. Under the forward bias conditions, the potential barrier is lowered. When the device is exposed to light, the direction of photo-voltage is contrary to the bias, which further lower the barrier height of the junction, therefore the forward current increases quickly. It is observed that behaviour of *n*-ZnO/*p*-Si junction in different light medium is different. Since the surface of ZnO is gradually depleted of oxygen upon exposure to light, a layer with increasing density of oxygen vacancies (donors) must be formed at the surface. In light ON condition, an oxygen vacancy will donate an electron. Thus, the effective doping at the surface should increase, gradually reducing the resistance between the device contacts, resulting in the observed increase of the conductivity. Such effective doping at the surface is bound to cause accumulation of electrons near the surface. When the light is turned off and sample is in ambient air atmosphere, atmospheric oxygen will react with the surface and the Zn-rich surface gradually oxidizes back slowly and reducing the photocurrent.[25] The photoelectric effect observed in the device is because of the light induced electron generation at the depletion region of the structure[26].

Further, *I-V* characteristics of laser photon irradiated *n*-ZnO/*p*-Si junctions were studied in three

Table 1 — Electrical parameters estimated from *I-V* characteristics for pristine and irradiated *n*-ZnO/*p*-Si junction.

Sample	Medium Condition	J_s (A/cm^2)	Turn on Voltage	N	If/Ir @ ±5v
Pristine n-ZnO/p-Si	Normal Light	1.5×10^{-4}	0.8	3.1	1.47×10^3
	Ultraviolet and Dark	2.1×10^{-5}	1.2	4.3	2.26×10^3
Irradiated n-ZnO/p-Si	Normal Light	5.0×10^{-5}	1.2	2.6	1.43×10^3
	Ultraviolet and Dark	5.0×10^{-5}	1.2	2.6	1.25×10^1 (under UV) 1.43×10^2 (under Dark)

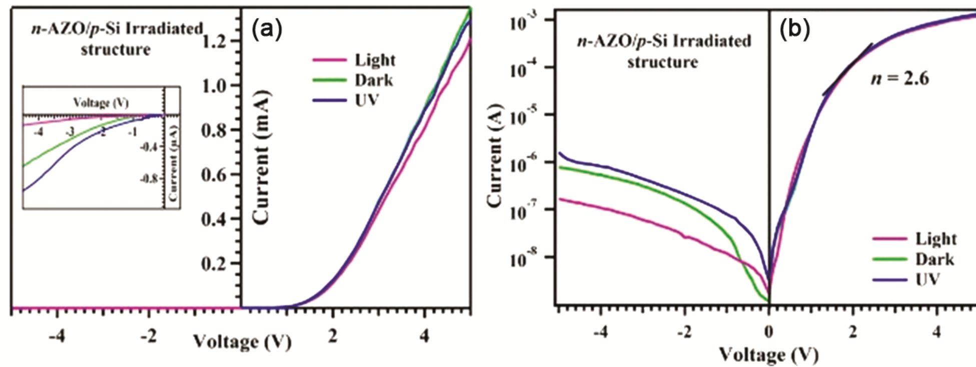

Fig. 6 — (a) *I–V* characteristics and (b) semi log *I-V* plot of laser irradiated *n*-ZnO/*p*-Si junction

different light conditions. The *I-V* characteristic of laser irradiated *n*-AZO/*p*-Si junction is shown in the fig. 6. Good rectifying and photoelectric behaviour were observed for the photon irradiated device. The dark leakage current is small, whereas its photocurrent generated under light is higher. Under reverse bias conditions, photocurrent caused by the *n*-ZnO /*p*-Si junction under light was larger than the dark current. After the laser irradiation, the threshold voltage was almost the same (1.2 V) for dark and UV illumination condition but it was increased from 0.8 to 1.2 V for normal light condition. Also, the leakage current was increased for reverse bias for all condition after laser irradiation. So, forward to reverse current ratio decreases after laser irradiation. The ideality factor for laser irradiated *p-n* junction was found to improve to a value of 2.6, which is same for all conditions. The calculated electrical parameters are shown in table 1. Although optimization of the laser irradiation intensity is needed; we demonstrated the change of the junction properties of the *n*-ZnO/*p*-Si device. The selective laser irradiation can be one of the effective techniques to improve the electrical *n*-ZnO/*p*-Si junction.These results show the possibility of using the fabricated junction for UV detector, photodetector, solar cell and gas sensor applications.

Conclusions

The *p-n* junction consisting of *n*-ZnO/*p*-Si was successfully fabricated by using PLD. The GIXRD revealed (100) oriented growth of AZO due to (100) orientation of *p*-Si substrate. The AFM and SEM analysis show the AZO film has uniform grain distribution and crack free surface. The stoichiometric elemental analysis of *n*-ZnO/*p*-Si junction was carried out by EDAX. The *I-V* characteristic of the *n*-ZnO/*p*-Si junction showed the rectifying property which confirms the proper formation of the *p-n* junction. The *n*-ZnO/*p*-Si junction showed variations in the photoelectric *I-V* characteristics under different light condition due to photovoltaic nature of the AZO thin film. The effect of the 532 nm laser light irradiation on the electrical parameters of *n*-ZnO/*p*-Si junction was demonstrated; with a considerable increase in the J_s values. It is concluded that *n*-ZnO/*p*-Si junction promising for its application as a photodiode that can detect UV and visible photons.

Acknowledgement

Authors are thankful to DST &UGC India for FIST & DRS-SAP projects respectively.

References

1 Dejam L,Mohammad E S, Nazari H H, Elahi H, Solaymani S & Ghaderi A, *J Mater Sci Mater Electron*, 27 (2016) 685.
2 Lu X H, Wang D, Li G R, Su C Y, Bin K D & Tong Y X, *J Phys Chem C*, 113 (2009) 13574.
3 Zhang L, Jin K, Li S, Wang L, Zhang Y & Li X, *J Electron Mater*, 44 (2015) 244.
4 Rakhshani A E, *J Appl Phys*, 108 (2010) 1.
5 Mridha S & Basak D, *J Appl Phys*, 101 (2007) 083102.
6 Jeong I S, Kim J H & Im S, *Appl Phys Lett*, 83 (2003) 2946.
7 Bedia F Z, Bedia A, Benyoucef B & Hamzaoui S, *Phys Proc*, 55 (2014) 61.
8 Prabhu R R, Saritha A C, Shijeesh M R & Jayaraj M K, *Mater Sci Eng B: Solid-State Mater Adv Technol*, 220 (2017) 82.
9 Mistry B V, Bhatt P, Bhavsar K H, Trivedi S J, Trivedi U N & Joshi U S, *Thin Solid Films*, 519 (2011) 3840.
10 Singh R & Soni R K, Elsevier Inc, 2019.
11 Mistry B V, Avasthi D K & Joshi U S, *Appl Phys A: Mater Sci Proc*, 122 (2016) 1.
12 Joshi U S, *Radiat Effects Defects Solids*, 166 (2011) 724.
13 Hewlett R M & McLachlan M A, *Adv Mater*, 28 (2016) 3893.
14 Sheehy M A, Tull B R, Friend C M & Mazur E, *Mater Sci Eng B: Solid-State Mater Adv Technol*, 137 (2007) 289.

15 Brown M S & Arnold C B, *Laser Precision Microfabricat*, 135 (2010) 91.
16 Chhaya U V, Mistry B V, Bhavar K H, Gadhvi M R, Lakhani V K, Modi K B & Joshi U S, *Indian J Pure Appl Phys*, 49 (2011) 833.
17 Mistry J, Mistry B V, Trivedi U N, Pinto R & U S Joshi, *AIP Conf Proc*, 1349 (2011) 725.
18 Chirakkara S & Krupanidhi S B, *Thin Solid Films*, 520 (2012) 5894.
19 Zinzuvadiya S, Pandya N C & Joshi U S, *Thin Solid Films*, 669 (2019) 525.
20 Dong B Z, Fang G J, Wang J F, Guan W J & Zhao X Z, *J Appl Phys*, 101 (2007).
21 Hashmi J Z, Siraj K, Naseem S & Shaukat S, *Mater Res Exp*, 3 (2016) 1.
22 Tauc J C, *Optical Properties of Solids*, Abeles, North Holland, Amsterdam, 1972.
23 Pierrt R F, *Semiconductor Device Fundamentals*, Wesley, 1996.
24 Lien W C, Tsai D S, Chiu S H, Senesky D G, Maboudian R, Pisano A P & He J H, *IEEE Electron Dev Lett*, 32 (2011) 1564.
25 Gurwitz R, Cohen R & Shalish I, *J Appl Phys*, 115 (2014) 033701.
26 Ootsuka T, Liu Z, Osamura M, Fukuzawa Y, Kuroda R, Suzuki Y, Otogawa N, Mise T, Wang S, Hoshino Y, Nakayama Y, Tanoue H & Makita Y, *Thin Solid Films*, 476 (2005) 30.